Yan et al., http://www.jgp.org/cgi/content/full/jgp.201110647/DC1



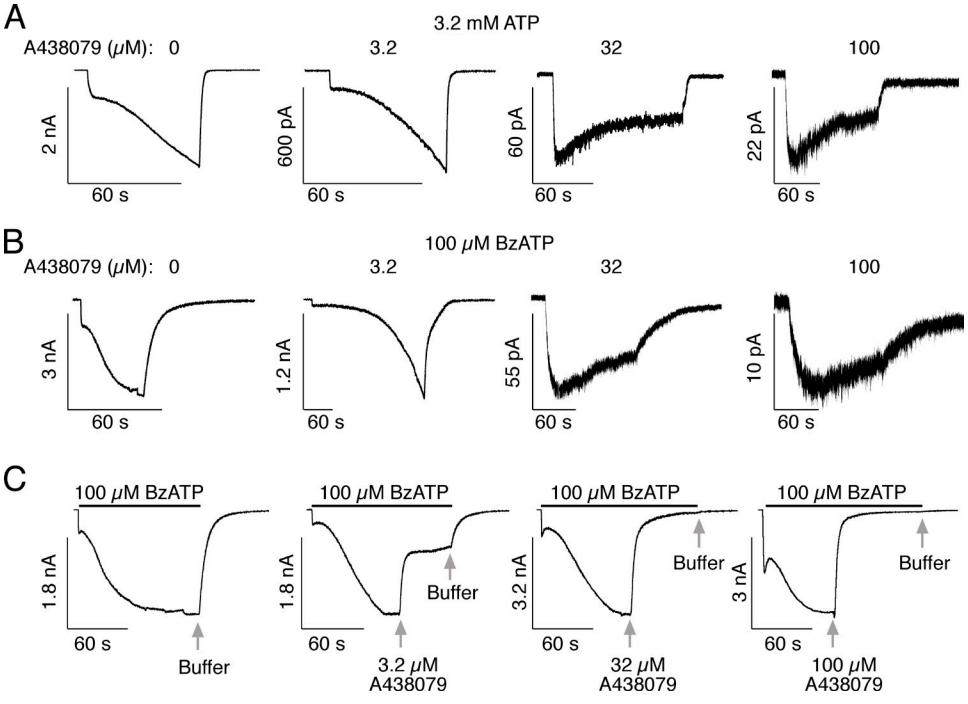


**Figure S1.** Effects of A438079, a P2X7R-specific antagonist, on agonist-induced receptor activation and deactivation. (A and B) Concentration-dependent effects of A438079 on ATP- (A) and BzATP (B)-induced current response. Note that the current scales are variable. At concentrations indicated above traces, mixture solutions of A438079 and agonist were applied. (C) Dose-dependent effect of A438079 on sustained BzATP-induced current.

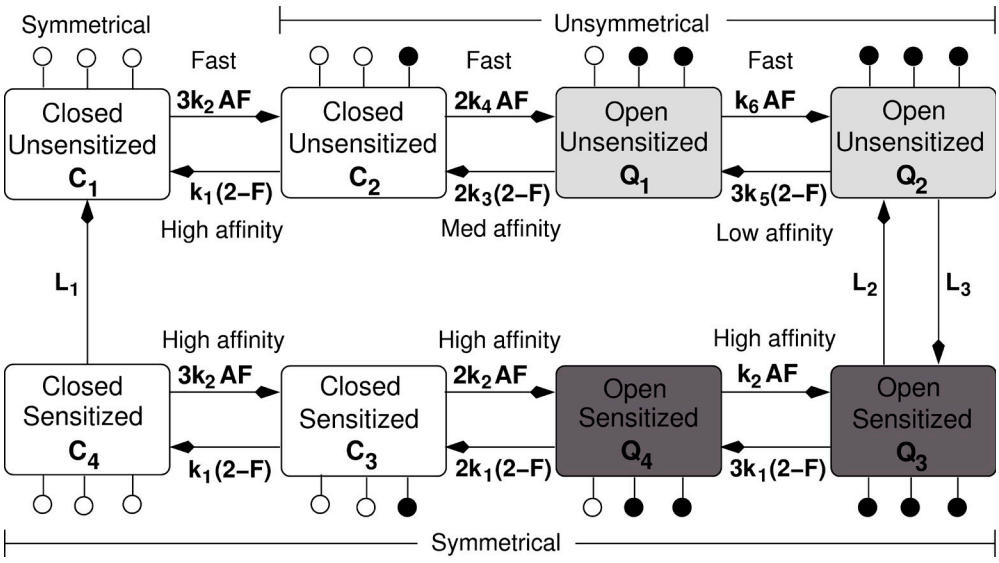


**Figure S2.** Markov state model adopted from the scheme in Yan et al. (2010) describing the binding and unbinding of agonist (ATP or BzATP) to the P2X7R. $C_1$–$C_4$ are closed states, whereas $Q_1$–$Q_4$ are open states, where $Q_1$ and $Q_2$ possess the same conductance $g_{12}$, whereas $Q_3$ and $Q_4$ possess the conductance $g_{34}$ ($g_{12} < g_{34}$). The open circles on each state represent unoccupied binding sites, whereas closed circles represent occupied binding sites. $C_1$, $C_2$, $Q_1$, and $Q_2$ are the unsensitized states, whereas $Q_3$, $Q_4$, $C_3$, and $C_4$ are the sensitized states. Negative cooperativity for agonist binding was assumed to occur only in the top row (unsensitized states). In other words, binding affinity decreases at each step in the top row (making agonist binding asymmetrical); i.e., $3k_2/k_1 > k_4/k_3 > k_6/3k_5$. Receptor sensitization was assumed to restore both symmetry and backward/forward rates to those belonging to the naive state $C_1$ (i.e., to $k_1$ and $k_2$). In other words, negative cooperativity is lost in the bottom row ($L_i$, i = 1–3, are the transition rates between unsensitized and sensitized states). The new feature added to this scheme is the inclusion of the allosteric binding of extracellular $Ca^{2+}$ to the receptor via the two fractions (Hill functions) $2 - F$, affecting the set of backward rates ($k_1$, $k_3$, and $k_5$), and $F$, affecting the set of forward rates ($k_2$, $k_4$, and $k_6$), both of which depend on the concentration of extracellular divalent cations $[DC]_e$, including $Ca^{2+}$.

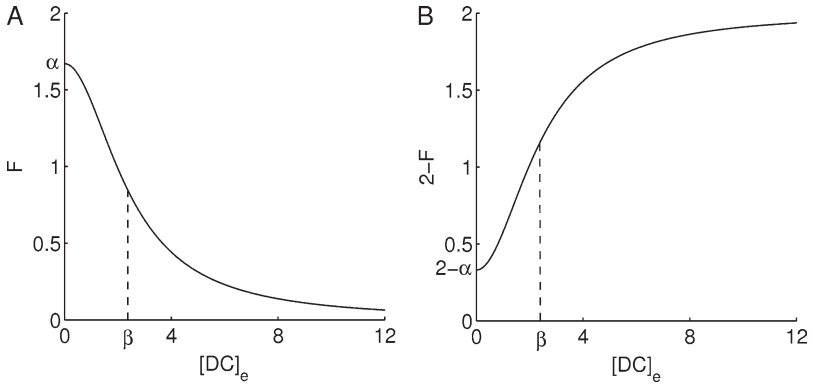


**Figure S3.** Fitted plots describing the effects of divalent cations. Graphs of the fractions $F = \alpha\beta^2/(\beta^2 + [DC]_e^2)$ (A) and $2 - F$ (B), the Hill functions describing the dependency of P2X7R allosteric regulation by the concentration of extracellular divalent cations $[DC]_e$ (specifically fitted to $Ca^{2+}$). β represents both the $IC_{50}$ for $F$ and $EC_{50}$ for $2 - F$, whereas α satisfies $F(0) = \alpha$.

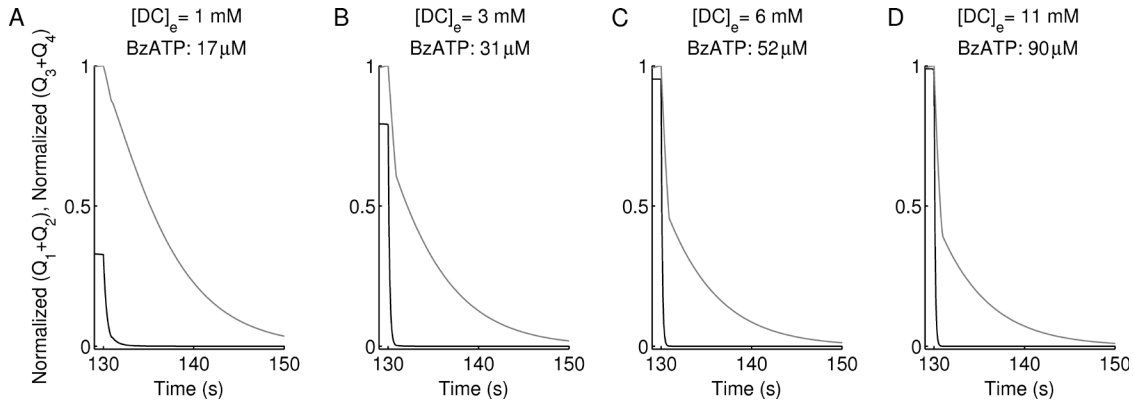


**Figure S4.** Deactivation phases of the open states $Q_1 + Q_2$ and $Q_3 + Q_4$, normalized by their maximum values, when a single naive model cell is activated by the same free BzATP concentration. This was achieved by simultaneously varying the concentrations of extracellular $Ca^{2+}$ and BzATP, specified by the values on top of each panel. B–D show that at higher $[DC]_e$, the slow component of the deactivation phase of the open state $Q_3 + Q_4$ gradually recedes in favor of the open state $Q_1 + Q_2$ when compared with A.

*Table S1*
*Parameter values and distributions used in modeling of P2X7R gating according to the scheme in Fig. S1 and Eqs. 1–9*

| Symbol | Parameter values and distributions | |
|---|---|---|
| | Values | Distribution |
| $k_1$ | 0.3 $s^{-1}$ | Normal, $\sigma = 0.003$ |
| $k_2$ | 40,000 $M.s^{-1}$ | Normal, $\sigma = 400$ |
| $k_3$ | 2.4 $s^{-1}$ | Normal, $\sigma = 0.024$ |
| $k_4$ | 50,000 $M.s^{-1}$ | Normal, $\sigma = 500$ |
| $k_5$ | 1.58 $s^{-1}$ | Normal, $\sigma = 0.0158$ |
| $k_6$ | 7,000 $M.s^{-1}$ | Normal, $\sigma = 70$ |
| $L_1$ | 0.0001 $s^{-1}$ | NA |
| $L_2$ | 0.004 $s^{-1}$ | Normal, $\sigma = 4 \times 10^{-5}$ |
| $L_3$ | 0.5 $s^{-1}$, 0.1 $s^{-1}$[a] | Normal, $\sigma = 0.005$ |
| $\alpha$ | 1.67 (unitless) | Normal, $\sigma = 0.0167$ |
| $\beta$ | $2.4 \times 10^{-3}$ M | Uniform, $[2\text{-}3] \times 10^{-3}$ |
| $g_{12}$ ($Q_1 + Q_2$ conductance) | $1.5 \times 10^{-8}$ S | Normal, $\sigma = 1.5 \times 10^{-10}$ |
| $g_{34}$ ($Q_3 + Q_4$ conductance) | $4.5 \times 10^{-8}$ S | Normal, $\sigma = 4.5 \times 10^{-10}$ |
| $V$ (holding potential) | $60 \times 10^{-3}$ V | NA |
| $E$ (reversal potential) | 0 V | NA |

NA, not applicable.
[a]This value was used only once to generate the second panels (counting from left) in Fig. 6 (A and B; see Yan et al. [2010] for more details).

## REFERENCES

Yan, Z., A. Khadra, S. Li, M. Tomic, A. Sherman, and S.S. Stojilkovic. 2010. Experimental characterization and mathematical modeling of P2X7 receptor channel gating. *J. Neurosci.* 30:14213–14224. http://dx.doi.org/10.1523/JNEUROSCI.2390-10.2010